European Polymer Journal 49 (2013) 3878–3888

Contents lists available at ScienceDirect

European Polymer Journal

journal homepage: www.elsevier.com/locate/europolj

Macromolecular Nanotechnology

Preparation and characterization of graphite nano-platelet (GNP)/epoxy nano-composite: Mechanical, electrical and thermal properties

Swetha Chandrasekaran [a,*], Christian Seidel [c], Karl Schulte [a,b]

[a] Institut für Kunststoffe und Verbundwerkstoffe, Technische Universität Hamburg-Harburg, Denickestrasse, 15, D-21073 Hamburg, Germany
[b] King Abdulaziz University, Jeddah, Saudi Arabia
[c] Siemens AG, Corporate Technology, Günther-Scharowsky-Strasse, 1, D-91050 Erlangen, Germany

ARTICLE INFO

Article history:
Received 10 June 2013
Received in revised form 28 September 2013
Accepted 9 October 2013
Available online 19 October 2013

Keywords:
Graphite nano-platelet/epoxy nano-composite
Three-roll milling technique
Fracture toughness
Thermal conductivity
Electrical conductivity
Fractography

ABSTRACT

Epoxy based polymer nano-composite was prepared by dispersing graphite nano-platelets (GNPs) using two different techniques: three-roll mill (3RM) and sonication combined with high speed shear mixing (Soni_hsm). The influence of addition of GNPs on the electrical and thermal conductivity, fracture toughness and storage modulus of the nano-composite was investigated. The GNP/epoxy prepared by 3RM technique showed a maximum electrical conductivity of 1.8×10^{-03} S/m for 1.0 wt% which is 3 orders of magnitude higher than those prepared by Soni_hsm. The percentage of increase in thermal conductivity was only 11% for 1.0 wt% and 14% for 2.0 wt% filler loading. Dynamic mechanical analysis results showed 16% increase in storage modulus for 0.5 wt%, although the Tg did not show any significant increase. Single edge notch bending (SENB) fracture toughens (K_{IC}) measurements were carried out for different weight percentage of the filler content. The toughening effect of GNP was most significant at 1.0 wt% loading, where a 43% increase in K_{IC} was observed. Among the two different dispersion techniques, 3RM process gives the optimum dispersion where both electrical and mechanical properties are better.

1. Introduction

Graphite nano-platelets (GNPs) are a new class of filler which consist of small stacks of graphene and are usually 1–15 nm thick. Compared with clay, they have a similar layered structure but with better mechanical properties. Generally, these graphite nano-platelets are prepared by intercalating graphite either with metal ions or by acid treatment. This is further exfoliated by thermal treatment to yield GNPs [1,2]. Similar to carbon nanotubes (CNTs), these two-dimensional layered structures also possess excellent electrical and thermal conductivities along with high modulus. However, the above mentioned properties strongly depend on the number of layers stacked in GNPs, the degree of crystallinity in the graphitic plane, their aspect ratio and the order of stacking [3,4]. Perhaps the most interesting application for this material is to use them as filler in composite structures. They have already shown promising results in the field of polymer composites as sensor, thermal interface materials and to create electrically conducting polymers [5,6]. Polymers are well known for their specific strength and flexibility but have poor fracture toughness. To overcome this shortcoming, often they are reinforced with micron-sized or nano-sized fillers like silica, nano-clay, carbon black (CB) and carbon nanotubes (CNTs) [7]. Similar to other polymer nano-composites, when used as filler in a polymer matrix, the glass transition temperature, modulus and fracture toughness of the polymer is improved upon addition of GNPs [8–10].

Though, CNTs are ideal for toughening the particles, one disadvantage is the increase in viscosity due to

* Corresponding author. Tel./fax: +49 (0)40 42878 4504.
E-mail address: Swetha.chandrasekaran@tuhh.de (S. Chandrasekaran).

0014-3057/$ - see front matter © 2013 Elsevier Ltd. All rights reserved.
http://dx.doi.org/10.1016/j.eurpolymj.2013.10.008

entanglement and high surface area of the tubes which affects the processing. Unlike CNTs, GNPs have a 2-D layered structure which has higher surface area enabling better stress transfer and also lower viscosity of the composite compared to CNTs during fabrication [11]. However, the already existing problem of dispersing the nanofillers in a polymeric matrix and improving the compatibility between the filler and matrix holds good for dispersing GNPs too. Owing to the large specific surface area, they are more prone to form agglomerates which in turn will affect the overall properties of the nano-composite [12,13]. The effect of the dispersion method on the properties of graphene/graphite nano-platelet composite and functionalization of the filler are being investigated extensively [14,15].

Investigations on the mechanical aspects of GNP/epoxy, pertaining to its fracture toughness and flexural modulus have shown significant improvement with an increase in the loading and are greatly dependent on the lateral flake size of the filler [16]. In another study on graphene epoxy composite at low filler content of 0.1 wt%, a noticeable increment of 31 wt% in modulus and 40% in fracture toughness was observed [17].

Thermal conductivities of GNP/silicone composite prepared by three-roll milling technique improved by 18% for 25 wt% loading of commercially available GNPs [18]. Comparing the thermal conductivities using different fillers like neat graphite, expanded graphite and graphene nano-platelets in an epoxy matrix, there was a marginal increase in thermal conductivity for GNPs and this value decreased as the filler content increased beyond 0.6 vol%. This is attributed to the poor dispersion of the filler [19,20]. Another study based on non-covalent functionalisation of graphene sheets dispersed in epoxy reported 800% increase in thermal conductivity for 4 wt% of filler loading. This is attributed to strong interaction between the matrix and filler, which reduces the interfacial thermal resistance and also homogeneous dispersion due to functionalisation [21].

The object of this work is to analyse the influence of addition of GNPs to epoxy matrix processed by three – roll milling technique, in terms of mechanical, thermal and electrical properties. To analyse the effect of processing technique on the electrical properties, an additional processing method was employed. This study gives an overview of the overall performance of the GNP/epoxy nano-composite prepared by 3RM technique.

2. Experimental methods

2.1. Preparation of the nano-composite

The graphite nano-platelets (GNPs) were purchased from Punto Quantico S.r.1® (Italy). The GNPs are prepared from graphite through metal intercalation followed by thermal treatment for exfoliation of the sheets. The GNPs have an average flake thickness of 12–15 nm and a lateral size of 20–50 μm as per the data sheet of the supplier. The matrix system is bisphenol A based epoxy resin Araldite LY556 cured with anhydride hardener Aradur 917 and imidazole accelerator DY 070, mixed at the weight ratio of 100:90:1 as per the datasheet of the supplier Huntsman®, Switzerland. The GNPs were dispersed in epoxy matrix using a three-roll mill from EXAKT® 120E (Advanced Technologies GmbH, Germany). The gap between the feed roll and the apron roll was varied from 120 μm down to 5 μm and the whole suspension was milled seven times in total in order to achieve a uniform dispersion.

The second dispersion method is sonication combined with high speed shear mixing technique, where the GNPs were sonicated in solvent (ethyl acetate) for 30 min to exfoliate the fillers. To this solvent/GNP slurry appropriate amounts of epoxy was added and then subjected to high speed shear mixing for 1.5 h at 11,000 rpm, which was simultaneously heated at 70 °C to remove solvent. For further removal of solvent, overnight heating in the oven at 70 °C was carried out.

The GNP/epoxy suspensions after 3RM process or Soni_hsm process was manually mixed with appropriate amounts of hardener and accelerator for 10 min, which was later degassed at 50 °C and then cured in oven for 80 °C – 4 h followed by post curing at 140 °C – 8 h. A schematic representing the preparation steps are presented in Fig. 1. Nano-composites with different weight percentage of the filler varying from 0.1 wt% to 2.0 wt% were prepared.

2.2. Characterization

Morphological characterization of the nano-composite as well as the suspension was done using scanning electron microscope (SEM) from LEO 1530 FE-SEM (Carl Zeiss, Germany) and light microscope (LM) from Leica Polyvar in transmission mode respectively. Prior to dispersion, the morphology of the as-received filler was observed using SEM and the quality of the GNPs was studied using Brucker AXS – D8 Advance X-ray diffractometer (XRD). The diffractograms were recorded from 15° to 65° with a step size of 0.02°, operating with Cu Kα radiation. Along with XRD, Raman spectroscopy was also done to ascertain the quality of the fillers.

The electrical properties were measured by means of impedance spectroscopy with two point contact. Three circular samples (15 mm diameter × 2 mm thickness) from each filler concentration covered with a silver paint (acts as electrodes) were tested. The measurements were carried out at a frequency range from 20 Hz to 1 MHz using a voltage of 1 V. For comparison, conductivity values at low frequency (200 Hz), comparable with the DC conductivity were taken.

The thermal diffusivity of GNP/epoxy composites was measured using the laser flash method, LFA-447 Nanoflash apparatus from NETZSCH, Germany at three different temperatures (30 °C, 50 °C and 100 °C). The samples were prepared in square-shaped forms of 10 mm × 10 mm and a thickness of 2 mm. Before testing, the samples were covered with graphite spray to ensure increased absorbance of flash energy on the front surface and emission of infrared light from the rear surface.

The investigation of the thermo-mechanical behaviour was performed using a Gabo Eplexor 500 N. For the measurements, a minimum of three rectangular samples of 40 mm × 2 mm × 2 mm dimensions were cut from the

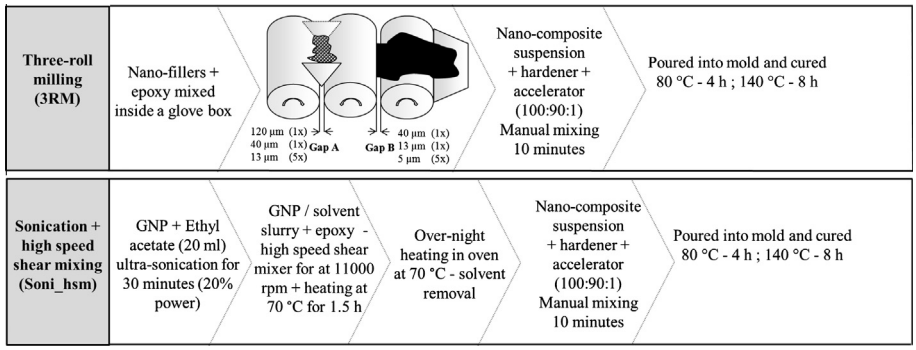

Fig. 1. Schematic of the different processing techniques employed to prepare GNP/epoxy nano-composite.

composite plate and ground. The tests were performed in tensile mode at a frequency of 10 Hz, with a dynamic strain of ±0.1%, within a temperature range between 20 °C and 200 °C with a heating rate of 3 °C/min.

Fracture toughness (K_{IC}) measurements were performed as per ASTM D5045-99 standard using single edge notch bending (SENB) specimens using Zwick universal testing machine. A minimum of 5 samples were tested in each system. The cross-head speed was 10 mm/min, and the length of the support span was 32 mm.

3. Results and discussion

3.1. Filler characterization

The SEM images of the as-received GNPs are shown in (Fig. 2a and b). It shows that, though the GNPs were subjected to thermal treatment for exfoliating the graphene sheets, there are agglomerates that are inevitable. The GNPs also have a wrinkled morphology (Fig. 2b) which is a result of thermal treatment.

The quality of the graphene sheets were analysed using XRD and Raman spectroscopy; the d-spacing of GNPs as well as the number of graphene layers stacked were calculated from Bragg and Scherer equations [22]. The X-ray diffractogram of the GNPs shown in Fig. 3, has a characteristic (002) peak positioned at 26.6° which corresponds to a d-spacing value of 3.35 Å which is close to the graphite d-spacing. The peak at 55° corresponds to the reflections from (004) planes. The full width at half maximum (FWHM) was calculated by fitting the curve using Lorentz function and Scherrer equation was used to calculate the crystallite thickness ($D_{0\ 0\ 2}$). Dividing the thickness with the d-spacing give a rough estimate of the number of layers, and in the present case it was found to be 170, which is much higher when compared to data given by the supplier (25 monolayers).

The Raman spectrum of a mono-layer graphene has two important peaks namely: G band that appears at 1580 cm^{-1} which is due to the in-place lattice motion of the carbon atoms; the second peak is the 2D band also known as the G' band – due to second order phonon process that appears at 2700 cm^{-1} (λ = 514 nm). This 2D band can also be used for the determination of number of layers [23]. It has been shown in the literature that the 2D band of a monolayer graphene can be fitted with a single Lorentzian peak, whereas a bi-layer is fitted with 4 such peaks indicating four double resonances. As the number of layers increases, this resonance process increases and converges to that of graphite which can be fitted with only 2 peaks. The Raman spectrum of as-received GNPs is shown in Fig. 4 was taken using a He–Ne laser. It can be clearly seen that the I_D/I_G ratio is smaller (0.16) which indicates that there are lattice defects in the material. The 2D band was fitted with two Lorentzian peaks, which is an indication that the number of graphene layers stacked in GNP is more than 10. However, the shoulder in the 2D band is not very prominent as visible in graphite. The $2D_1$ and $2D_2$ bands of the two fitted Lorentzian peaks for the GNPs are at 2654 cm^{-1} and 2689 cm^{-1} which is slightly different when compared to the bulk highly oriented pyrolytic graphite (HOPG) ($2D_1$ = 2690 cm^{-1} and $2D_2$ = 2720 cm^{-1}) from literature [24].

3.2. Morphological characterization of GNP/epoxy nano-composite

The dispersion of GNPs in epoxy after the milling process was observed under light microscope for the nano-composite suspensions. A small drop of suspension was placed on the glass slide and a cover slip was placed on it. The transmission light microscopic images of the suspension clearly show the formation of re-agglomerates in the suspension. Adequate dispersion of the agglomerates was achieved at 0.3 wt%, where the conducting networks start to form; the percolation cluster formation is clearly visible in Fig. 5c. This conducting network becomes denser as the filler content is doubled (Fig. 5d).

On the other hand, Fig. 5e–g represents the optical micrographs of suspensions prepared by sonication with shear mixing. Before analysing the dispersion it must be noted that in this case, the use of solvent must be considered. After the solvent removal step, the amount of remnant solvent in the suspension was found to be (1–2%) in the composite suspension which was measured using thermo-gravimetric analysis (Supplementary information). The presence of solvent can affect the viscosity of the resin and thereby also the dispersion state. It is very evident from the micrographs that the GNPs in the suspension prepared via Soni_hsm have bigger agglomerates [25]. Unlike the 3RM

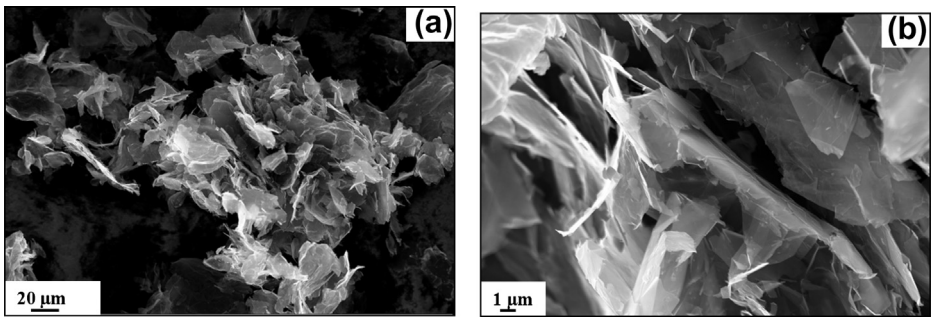

Fig. 2. Scanning electron micrographs of as-received GNPs (a) agglomerates of the particles and (b) wrinkled, stacked graphene layers.

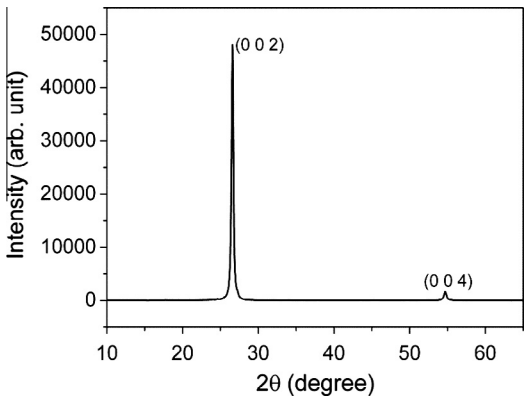

Fig. 3. X-ray diffractogram of as-received GNPs.

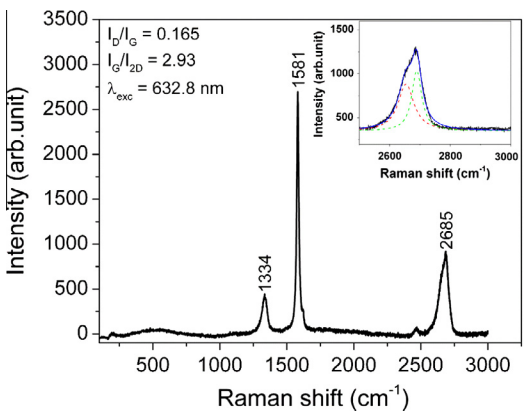

Fig. 4. Raman spectra of G and 2D bands of as-received GNPs (He–Ne laser excitation).

process, there are only a few percolated networks. This partly explains that the sonication with high speed shear mixing process produces nano-composite suspensions with lesser exfoliation (thicker GNPs) compared to those prepared by 3RM process.

Apart from analysing the distribution of fillers in the epoxy matrix, the aspect ratio of the fillers after dispersion can be calculated using simple models through rheological measurements. After the dispersion using three-roll mill the viscosity of the composite suspension as a function of shear rate and filler content were measured (see Supplementary information). The rheology of a particle suspension depends on physical properties and of processes that occur within the suspended particles. The most important factors are particle volume fraction φ, particle shape, interactions between particles, and the spatial arrangement of particles [26]. There are several empirical formulas that connect the viscosity to aspect ratio and one such equation was developed in 1959 by Krieger and Dougherty relates the viscosity to volume fraction of filler is shown in the following equation [27].

$$\eta_r = \left(1 - \frac{\varphi}{\varphi_m}\right)^{-B\varphi_m} \quad (1)$$

where η_r is the relative viscosity; φ is the volume fraction of the filler and B is called the Einstein's co-efficient and the product $B\varphi_m$ equals 2.

For particles of arbitrary shape, it was found that the fitting parameter φ_m depends on the aspect ratio rp of the filler through the following equation:

$$\varphi_m = \frac{2}{0.321rp + 3.02} \quad (2)$$

Combining Eqs. (1) and (2) the aspect ratio of GNP fillers dispersed in the epoxy matrix using 3RM technique was found to vary between 200 and 300. This obtained value is much less than the values reported in literature [28]. The fitting curves and the viscosity of the suspensions are given in the Supplementary information. Since the aspect ratio of the filler is much lower, a very drastic increase in the properties of the composite cannot be expected. This also shows that a lower percolation threshold in terms of electrical conductivity for this system cannot be achieved. However, the degree of dispersion and the spatial distribution of GNPs in epoxy matrix prepared by two different methods can be understood from the cryo-fractured surfaces of the cured composite and are shown in Fig. 6. The higher surface roughness of GNP/epoxy (3RM) sample shows better dispersion of GNPs than those from Soni_hsm. This was also visible in the optical micrographs of the uncured suspension which shows that this dispersion state is mainly due to the process.

In order to investigate the dispersion quality and the dispersion of the filler in detail for samples produced by 3RM process, 500 nm thin slices were cut from the cured

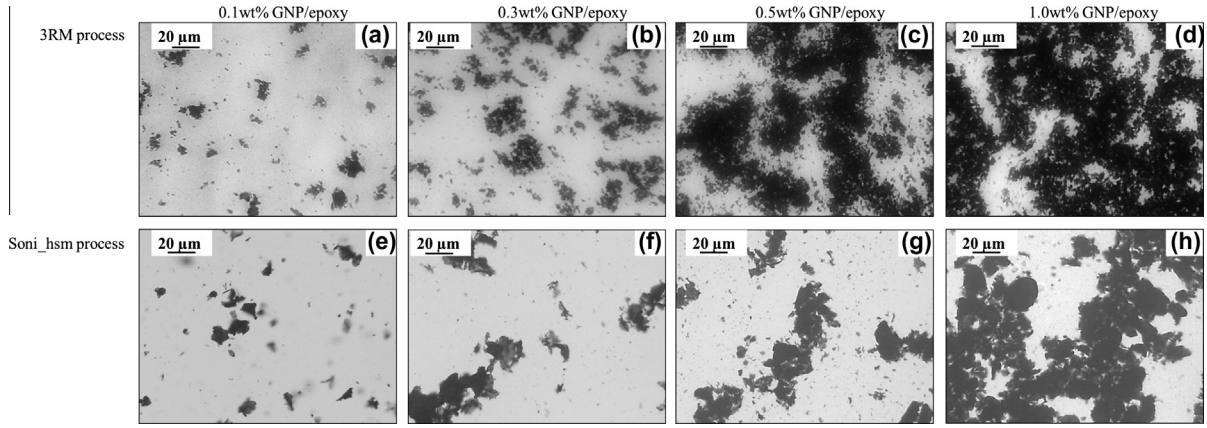

Fig. 5. Transmission light microscopic images of GNP/epoxy suspension prepared by (a-d) 3RM process for 0.1-1.0 wt% and (e-h) Soni_hsm process for 0.1-1.0 wt% respectively.

composite using an ultra-cut microtome, and then placed on Si wafer. The microstructure of the cured GNP/epoxy (3RM) composite is presented in Fig. 7. It can be seen that a fairly uniform distribution is achieved using the three-roll milling technique, also the number of GNP particles or agglomerates increases with filler content (Fig. 7a, c and e). In the case of 2.0 wt% GNP/epoxy (Fig. 7e) there are still some primary agglomerates which are densely packed agglomerates, proving the difficulty to overcome the high adhesive force (van der Waals) despite the enormous shear force applied via three-roll milling [29]. A large number of secondary agglomerates, which is a GNP rich region in epoxy consisting of either well-dispersed GNP sheets or a few layered GNPs (Fig. 7f), are also observed. In Fig. 7b, the exfoliation (gap) between the graphitic layers can be seen; whereas in Fig. 7d, two primary agglomerates come in contact with each other forming a percolated network may result in electrical conductivity or charge transfer between the graphene sheets.

3.3. Electrical conductivity of GNP/epoxy nano-composite

The electrical conductivity of the nano-composite as a function of filler content for two different preparation method is presented in Fig. 8; it can be seen that for GNP/epoxy (3RM) samples the conductivity increases by 5 orders of magnitude at 0.3 wt%. It continues to increase up to 0.5 wt% where the conductivity is of the order of $\sim 2 \times 10^{-03}$ S/m and reaches a plateau at 2.0 wt%. However, as observed in carbon nanotube or carbon black filled epoxies, in this case the conductivity does not remain constant but increases to 5.8×10^{-03} S/m. On the other hand, samples prepared using Soni_hsm process exhibits lesser conductivity. A maximum conductivity of 1×10^{-06} S/m was achieved at 1.0 wt% and this is 3 orders of magnitude lower than the samples prepared using 3RM technique. However, no prominent S-curve as expected according to percolation theory was observed for Soni_hsm and the electrical conductivity values continue to show an increasing trend. This observation is very much in relation with the observed optical micrographs of the suspensions where visible network formation is observed at 0.5 wt%.

Clearly, Fig. 8 shows that the electrical conductivity of the nano-composite (GNP/epoxy_3RM) follows the percolation theory. The percolation threshold where the conductivity increases to 4 orders of magnitude is achieved at 0.3 wt%. The increase in conductivity at 0.3 wt% can be easily correlated to the observed micrographs of the suspen-

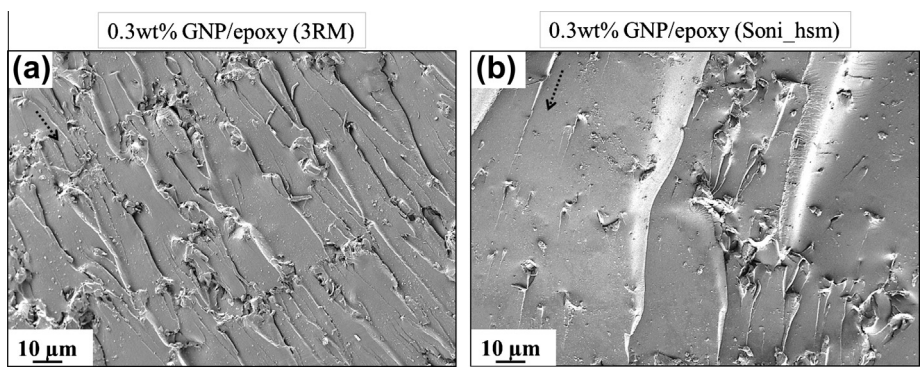

Fig. 6. Cryo-fractured SEM images of GNP/epoxy suspension (a) 0.3 wt% prepared by 3RM technique; (b) 0.3 wt% prepared by Soni_hsm technique respectively.

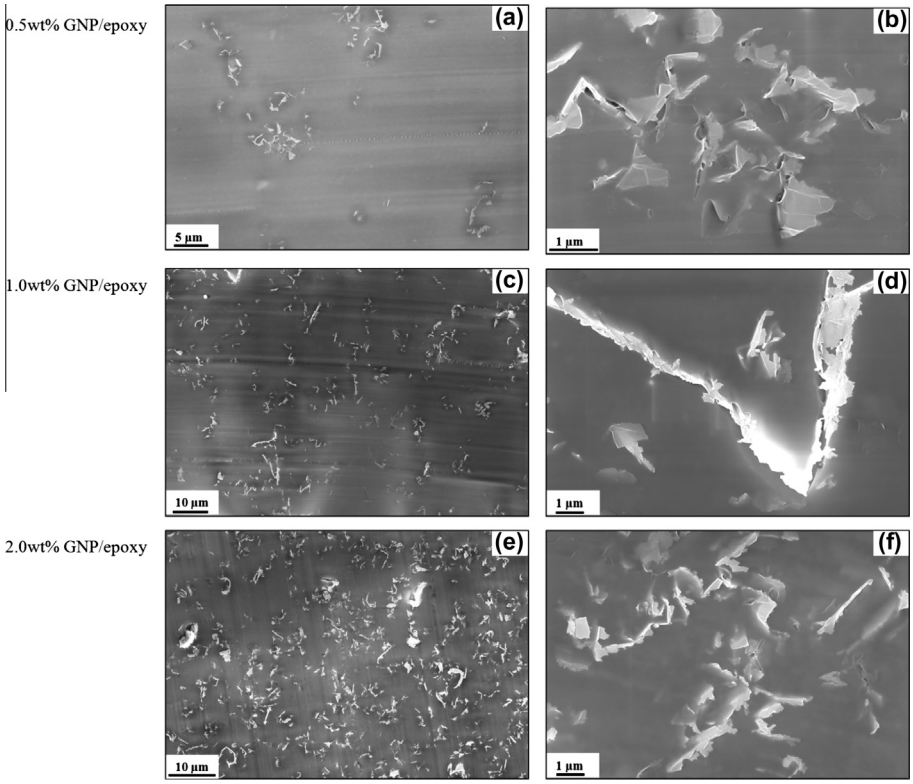

Fig. 7. Scanning electron microscopic images of GNP/epoxy slices on Si wafer (a & b) 0.5 wt%; (c & d) 1.0 wt%; (e & f) 2.0 wt% respectively.

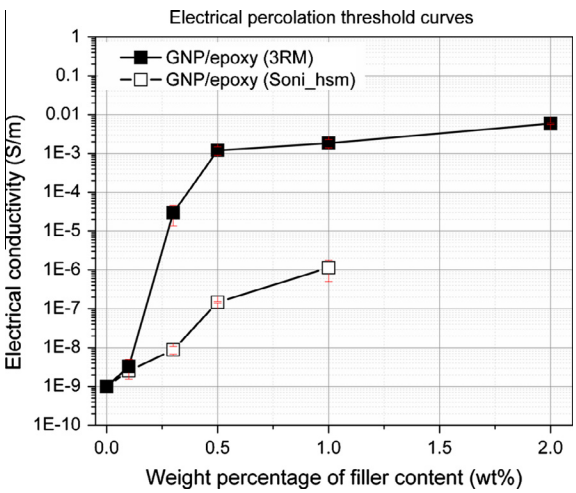

Fig. 8. Electrical conductivity of GNP/epoxy nano-composite as a function of weight percentage of the filler.

sion where the early formation of the conducting network occurs at 0.3 wt%. The percolation threshold for GNP/epoxy is higher than for carbon nanotube/epoxy composites (φ_c = 0.01 wt% for carbon nanotube/epoxy). This higher value of observed φ_c is due to the geometry of the filler (2D in case of GNPs) and the better dispersion ability of GNPs which is later reflected in the mechanical properties [30,31]. The ability of GNPs to shear between the graphitic layers makes it difficult to form a conductive network, unlike carbon nanotubes, which entangle with each other which results in a conductive network. Since the GNP/epoxy nano-composite produced by 3RM showed better electrical properties when compared to those produced by Soni_hsm, further analysis were focussed on the samples prepared using 3RM technique.

3.4. Thermal conductivity of GNP/epoxy nano-composite

The thermal conductivity of the GNP/epoxy samples as function of weight percentage of GNPs at three different temperatures were measured and are shown in Fig. 9. Each sample was tested 5 times at each temperature and the standard deviation was <1% and hence not represented in the figure. As expected the thermal conductivity increases with increase in temperature, which is a common trend exhibited by epoxy resins below their Tg. As seen from Fig. 9, the thermal conductivity increases by 6% for 1.0 wt% and is doubled to 14% for 2.0 wt% filler loading at 30 °C, although there is a drop in the thermal conductivity for 0.3 wt%. This increase of 14% at 2.0 wt% is very much in accordance with the values that are reported in literature [32].

The decrease in thermal conductivity occurs at 0.3 wt% (which is also the electrical percolation threshold) and a steep increase of thermal conductivity is observed between 0.3 wt% and 0.5 wt%. This initial drop and subsequent increase is mainly because of two effects which affects the heat flow in the system. Addition of filler in the matrix also creates an interfacial layer in which the phonon scattering reduces the heat flow and this effect

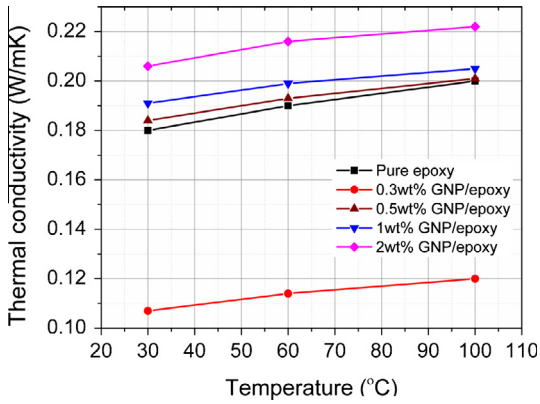

Fig. 9. Thermal conductivity of GNP/epoxy nano-composite as a function of weight percentage of the filler.

dominates when the filler content is 0.3 wt%. Beyond 0.3 wt%, addition of fillers, increases the volume of filler which has high thermal conductivity and hence the overall conductivity of the nano-composite increases. Unlike the electrical conductivity no percolation curve was observed for thermal conductivity. In the case of electrical conductivity the clusters formed by the electrically conductive fillers alone contribute to the overall conductivity and there is no matrix contribution. But, thermal conductivity is a concept based on phonons and both filler and matrix contribute to the heat flow. Since the difference in thermal conductivity of the filler and matrix is very high, the presence of large interfacial thermal resistance leads to the lack of percolation curve in thermal conductivity.

Since the effective heat propagation is due to acoustic phonons, a well-dispersed network of GNPs in the matrix at higher filler loadings (reduces the mean free path of heat carriers) contributes to the increased thermal conductivity with filler content. However, several factors such as aspect ratio of the filler, the intrinsic crystallinity of the graphitic layers, dispersion of GNPs, bonding between GNPs and epoxy and interfacial thermal resistance between the filler and matrix affects the thermal conductivity of the nano-composite [33]. To obtain a further enhancement in the thermal conductivity either the dispersion method needs to be modified or the filler content must be increased. Increasing the filler has its toll on the viscosity of the resin and makes the processing difficult. On the other hand, changing the dispersion method with the use of solvent alters the resin but other properties like electrical conductivity decreases. Without compromising on the resin properties and other physical properties of the nano-composite, the other solution is to combine CNTs and GNPs. The current focus of research is now on the hybrid systems where both CNTs and GNPs are combined to form a 3D-network, (CNTs bridge the GNPs) and an efficient phonon scatter occurs and a synergetic effect is observed for through plane conductivity [34–36].

3.5. Dynamic mechanical analysis (DMA)

The influence of temperature on storage modulus and loss factor ($\tan\delta$) of the GNP/epoxy nano-composite with different weight percentage of the filler is presented in Fig. 10a and b; Table 1 contains the storage modulus in glassy and rubbery state, height of the $\tan\delta$ peak and Tg (measured from $\tan\delta$ peak). The good reproducibility of data having only 2% error is an indication for the dispersion quality achieved using three-roll milling technique. The Tg of the composite had only a marginal increase of 3 °C which is related to high cross-linking density of the thermosetting epoxy. A maximum increase of 15% in the storage modulus (E'_r) was obtained at 0.5 wt% filler and upon addition of filler to 2.0 wt% the increase in storage modulus (E'_r) remained the same. In general, the extent of interaction between the matrix and filler is correlated to the "rubbery plateau" of storage modulus. Whereas, the height and peak position of loss factor ($\tan\delta$) relate to the cross linking density and mobility of polymeric chains. The higher glassy storage modulus, lower loss factor and higher Tg are associated with higher crosslink density and lower mobility of epoxy chains and, as a result, can indicate to a stronger bonding and load transfer at the filler–epoxy interface [37–39]. There was an anomalous behaviour observed at 0.5 wt% where the E'_r of 0.5 wt% is lower than the remaining filler content; the $\tan\delta$ peak is broader and has higher glassy storage modulus (E'_g). The measurement on this particular sample was repeated several times and all resulted in same behaviour. On comparing the E'_r of the pure epoxy

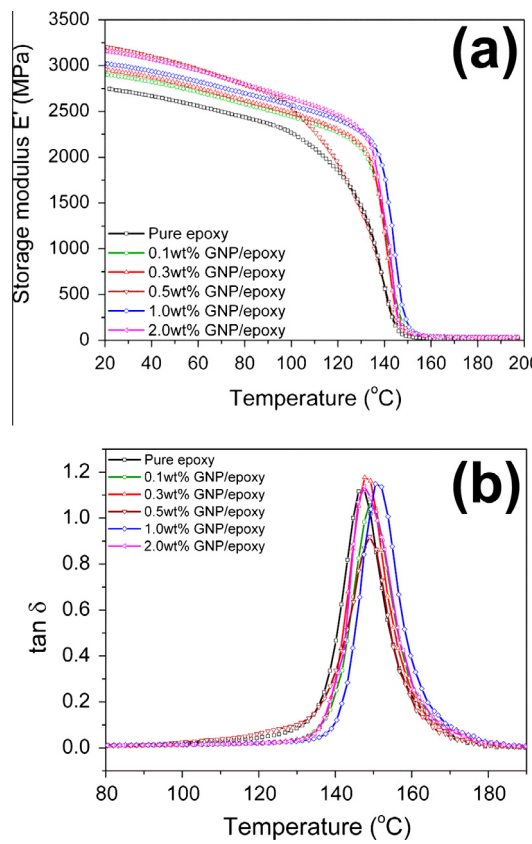

Fig. 10. Dynamic mechanical properties of GNP/epoxy (3RM) composite (a) storage modulus as function of temperature and (b) loss factor for varying filler content.

Table 1
Thermo-mechanical properties of GNP/epoxy composite tested.

Sample	Storage modulus (E'_g) at 25 °C in GPa	Rubbery modulus (E'_r) at 180 °C in GPa	Loss factor tan δ_{max}	Glass transition temperature Tg in °C (measured from tan δ peak)
Pure epoxy	2.75 ± 0.05	19.9 ± 1.0	1.12 ± 0.02	148
0.1 wt% GNP/epoxy	2.89 ± 0.05	27.10 ± 0.19	1.07 ± 0.03	149
0.3 wt% GNP/epoxy	2.94 ± 0.01	29.11 ± 0.31	1.18 ± 0.03	148
0.5 wt% GNP/epoxy	3.18 ± 0.04	23.43 ± 1.9	0.92 ± 0.03	149
1.0 wt% GNP/epoxy	3.01 ± 0.04	32.35 ± 0.08	1.15 ± 0.01	151
2.0 wt% GNP/epoxy	3.14 ± 0.07	34.37 ± 0.4	1.14 ± 0.02	148

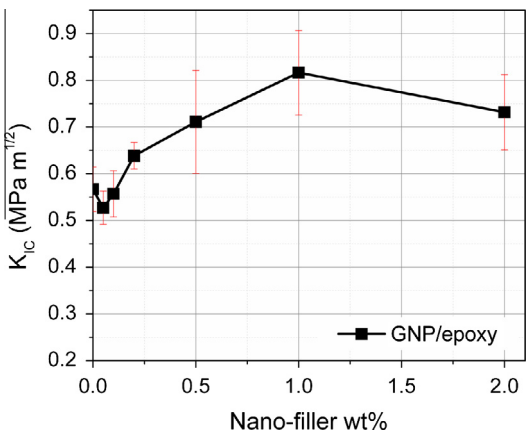

Fig. 11. Effect of GNP concentration on the fracture toughness of GNP/epoxy nano-composite.

with GNP/epoxy nano-composite, the E'_r increases which shows strong interaction between the filler and matrix [40]. However, the rubbery modulus of 0.5 wt% is lower when compared to other weight percentage of filler. This could indicate that a rheological percolation is achieved in this system at 0.5 wt%. This implies that a percolated network of GNPs is formed which in turn reduces the mobility of polymer chains and hence decreases the height of tan δ peak. When compared to pure epoxy, the rubber modulus E'_r increased to 72% which shows stronger interactions between the filler and the polymeric matrix which implies higher degree of crosslinking of the nanotube-reinforced epoxy.

3.6. Fracture toughness (K_{IC}) by 3-point bend tests

The fracture toughness (K_{IC}) was evaluated by three point end notch bending (3P-ENB) test. The 3P-ENB test was carried out mainly according to ASTM E397. Rectangular specimens were cut from the cured plates and were polished down to the dimension required for testing. The dimensions of the specimen were 36 mm (length) × 8 mm (height) × 4 mm (thickness). The distance between the supporting rollers of the 3 point bending test was 32 mm. The crosshead speed was 10 mm/min. The initial notch was introduced by rotating diamond coating blade

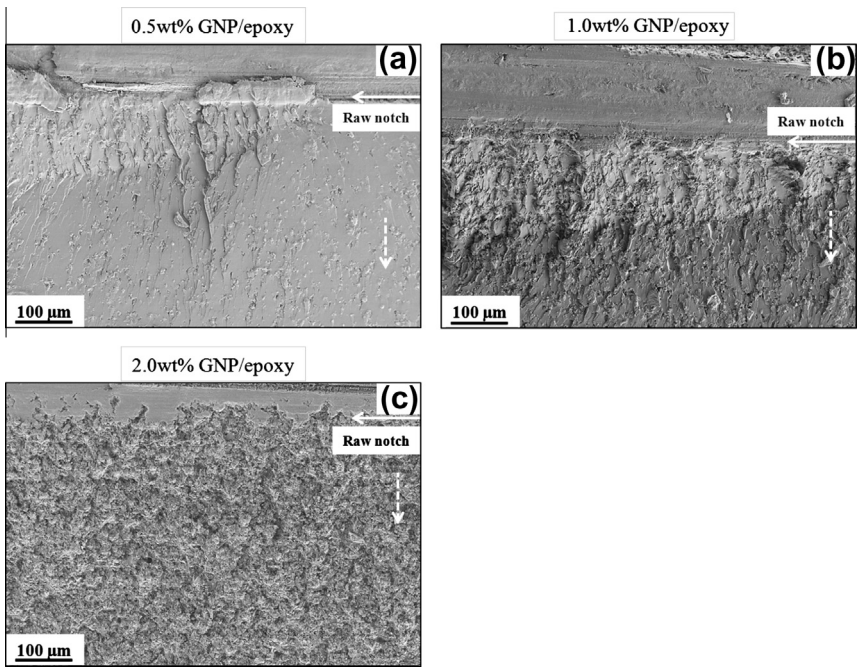

Fig. 12. Fractured surface of GNP/epoxy at lower magnification from the raw notch (a) 0.5 wt%; (b) 1.0 wt% and (c) 2.0 wt% with dotted arrow indicating the crack propagation direction.

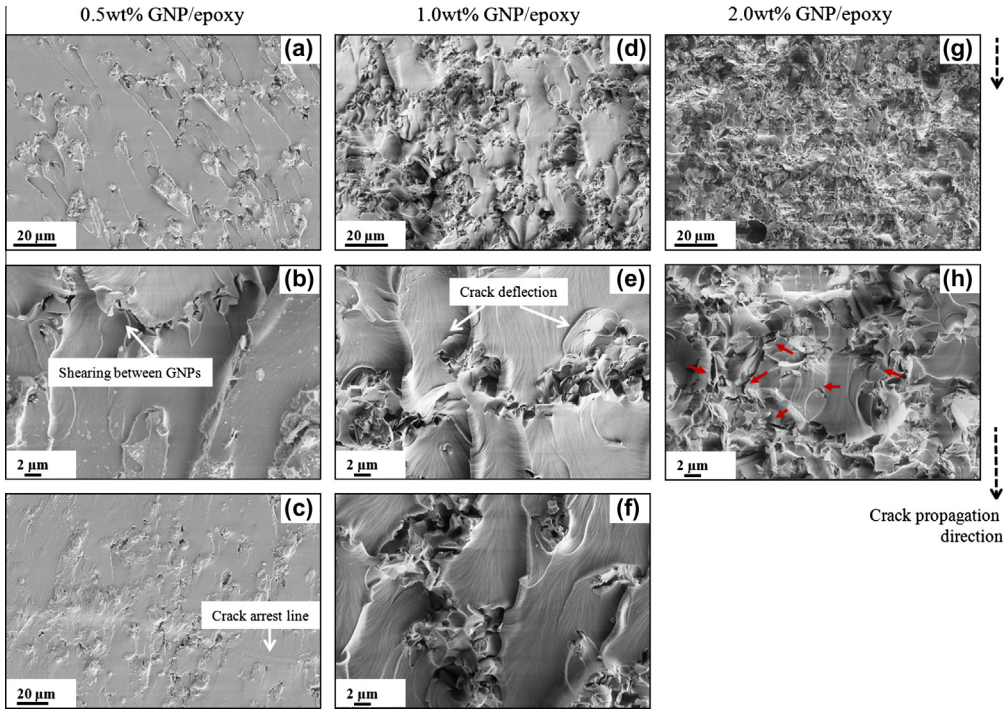

Fig. 13. Fracture surface of GNP/epoxy at higher magnification reveals (a, d and g) increase in surface roughness; (c) crack arrest lines; (e, f and h) crack deflection and inter-cleavage between the graphitic layers causing micro-cracks (red arrows (h)). (For interpretation of the references to colour in this figure legend, the reader is referred to the web version of this article.)

(thickness 0.6 mm) and was later sharpened to get a V-notch by sliding a razor blade. A minimum of 5 specimens were evaluated for each composite. The fracture toughness of the sample as a function of weight percentage of the filler is presented in Fig. 11.

The K_{IC} slightly decreases from its initial value from that of pure epoxy by 1.7% until 0.1 wt% of filler. Upon further increase in the concentration of the filler, the K_{IC} increases up to 43% and reaches a maximum at 1.0 wt% and for 2.0 wt% the values start to decrease. It is expected that beyond a certain weight percentage, the properties will decrease owing to the agglomerate formation of the nanoparticles. Fractographic studies were carried out on the samples to explain the observed increase in fracture toughness using scanning electron microscope. Fig. 12 shows the fracture surface of a GNP/epoxy composite (0.5 wt%, 1.0 wt% and 2.0 wt%) and the initial cracks originating from the raw notch are clearly visible in Figs. 11a and b. Unlike neat epoxies, the fracture surface of the GNP/epoxy is rough and this roughness increases with filler content. The observed surface roughness is due to tilting and twisting of the cracks and this should lead to an increase in the K_{IC}. However, the fracture toughness starts to decrease for 2.0 wt% GNP/epoxy samples while their fracture surface is extremely rough.

Upon further investigations at higher magnifications, shearing among the GNP agglomerates/sheets and crack arrest lines at the end of the samples were clearly visible (Fig. 13b and c). There was no evidence of de-bonding of the GNPs from the matrix, but several micro-cracks were observed. The GNPs acts as stress concentrators and creates many micro-cracks (Fig. 13h) which in turn increases the fracture surface area due to crack deflection [41,42]. The graphite nano-platelets are rigid and well bonded with the matrix, they did not yield to crack but instead deflected them (Fig. 13e) [43]. The weak interlayer forces between the graphitic layers are responsible for the interlayer delamination (Fig. 13h indicated in red arrow), thus giving rise to micro-cracks originating from within the graphitic layers [44].

4. Conclusions

The GNPs are an effective reinforcement for epoxies in terms of mechanical properties. A fairly uniform dispersion of the filler was achieved using both the three-roll milling and sonication combined with high speed shear mixing technique. However, GNP/epoxy nano-composite prepared via 3RM technique showed almost 3 orders of magnitude higher electrical conductivity than those prepared via Soni_hsm process. Hence, further characterization of the GNP/epoxy nano-composite in terms of mechanical and thermal properties were carried out the samples prepared via 3RM technique only. In the case of electrical conductivity, a minimum amount of GNPs for a percolation threshold is required rather than a homogenous dispersion, so that a valid conduction pattern is created along the matrix. Though the electrical conductivity of GNP/epoxy (3RM) composite reaches 5.8×10^{-03} S/m at 2.0 wt%, and the

percolation threshold is 0.3 wt% which is much higher when compared to carbon nanotube epoxy composite. This is possible in epoxy at very low loadings because of extremely high dispersive surface energy of nanoparticles which produce a spontaneous re-agglomeration. Thermal conductivity of the nano-composite did not increase more than 14% for 2.0 wt% of filler. The effective mechanical reinforcement was achieved for 0.5 wt% with 17% increase in glassy storage modulus and beyond this filler content not much increase in modulus was observed. A considerable increase in fracture toughness of 43% was obtained for 1.0 wt% filler loading. The incorporation of graphite nano-platelets toughness the epoxy matrix through crack deflection and by delamination in-between the graphitic layers causing micro-cracks.

Acknowledgement

The authors would like to acknowledge Mr. Varun Gopal student assistant, for his support in sample production and characterization. We would like to acknowledge DAAD-SIEMENS A/10/71620 scholarship for the financial support.

Appendix A. Supplementary material

Supplementary data associated with this article can be found, in the online version, at http://dx.doi.org/10.1016/j.eurpolymj.2013.10.008.

References

[1] Viculis LM, Mack JJ, Mayer OM, Hahn HT, Kaner RB. Intercalation and exfoliation routes to graphite nanoplatelets. J Mater Chem 2005;15(9):974.
[2] Geng Y, Wang SJ, Kim J. Preparation of graphite nanoplatelets and graphene sheets. J Colloid Interface Sci 2009;336(2):592–8.
[3] Zhang Y, Gu Y. Mechanical properties of graphene: effects of layer number, temperature and isotope. Computat Mater Sci 2013;71:197–200.
[4] Tong X, Wang H, Wang G, Wan L, Ren Z, Bai J, et al. Controllable synthesis of graphene sheets with different numbers of layers and effect of the number of graphene layers on the specific capacity of anode material in lithium-ion batteries. J Solid State Chem 2011;184(5):982–9.
[5] Sengupta R, Bhattacharya M, Bandyopadhyay S, Bhowmick AK. A review on the mechanical and electrical properties of graphite and modified graphite reinforced polymer composites. Prog Polym Sci 2011;36(5):638–70.
[6] Young RJ, Kinloch IA, Gong L, Novoselov KS. The mechanics of graphene nanocomposites: a review. Compos Sci Technol 2012;72(12):1459–76.
[7] Johnsen B, Kinloch A, Mohammed R, Taylor A, Sprenger S. Toughening mechanisms of nanoparticle-modified epoxy polymers. Polymer 2007;48(2):530–41.
[8] Li B, Zhong W. Review on polymer/graphite nanoplatelet nanocomposites. J Mater Sci 2011;46(17):5595–614.
[9] Yasmin A, Daniel IM. Mechanical and thermal properties of graphite platelet/epoxy composites. Polymer 2004;45(24):8211–9.
[10] Kuilla T, Bhadra S, Yao D, Kim NH, Bose S, Lee JH. Recent advances in graphene based polymer composites. Prog Polym Sci 2010;35(11):1350–75.
[11] Martin-Gallego M, Bernal M, Hernandez M, Verdejo R, Lopez-Manchado M. Comparison of filler percolation and mechanical properties in graphene and carbon nanotubes filled epoxy nanocomposites. Eur Polym J 2013;49(6):1347–53.
[12] Tang L, Wan Y, Yan D, Pei Y, Zhao L, Li Y, et al. The effect of graphene dispersion on the mechanical properties of graphene/epoxy composites. Carbon 2013;60:16–27.
[13] Li J, Sham M, Kim J, Marom G. Morphology and properties of UV/ozone treated graphite nanoplatelet/epoxy nanocomposites. Compos Sci Technol 2007;67(2):296–305.
[14] Raza M, Westwood A, Stirling C. Effect of processing technique on the transport and mechanical properties of graphite nanoplatelet/rubbery epoxy composites for thermal interface applications. Mater Chem Phys 2012;132(1):63–73.
[15] Li J, Vaisman L, Marom G, Kim J. Br treated graphite nanoplatelets for improved electrical conductivity of polymer composites. Carbon 2007;45(4):744–50.
[16] Chatterjee S, Nafezarefi F, Tai N, Schlagenhauf L, Nüesch F, Chu B. Size and synergy effects of nanofiller hybrids including graphene nanoplatelets and carbon nanotubes in mechanical properties of epoxy composites. Carbon 2012;50(15):5380–6.
[17] Rafiee MA, Rafiee J, Wang Z, Song H, Yu Z, Koratkar N. Enhanced mechanical properties of nanocomposites at low graphene content. ACS Nano 2009;3(12):3884–90.
[18] Raza M, Westwood A, Brown A, Stirling C. Texture, transport and mechanical properties of graphite nanoplatelet/silicone composites produced by three roll mill. Compos Sci Technol 2012;72(3):467–75.
[19] Esposito Corcione C, Maffezzoli A. Transport properties of graphite/epoxy composites: thermal, permeability and dielectric characterization. Polym Test 2013;32(5):880–8.
[20] Lin C, Chung D. Graphite nanoplatelet pastes vs. carbon black pastes as thermal interface materials. Carbon 2009;47(1):295–305.
[21] Teng C, Ma CM, Lu C, Yang S, Lee S, Hsiao M, et al. Thermal conductivity and structure of non-covalent functionalized graphene/epoxy composites. Carbon 2011;49(15):5107–16.
[22] Seung Hun H, Hae-Mi J, Sung-Ho C. X-ray diffraction patterns of thermally-reduced graphenes. J Korean Phys Soc 2010;57(61):1649.
[23] Ferrari AC, Meyer JC, Scardaci V, Casiraghi C, Lazzeri M, Mauri F, et al. Raman spectrum of graphene and graphene layers. Phys Rev Lett 2006;97(18).
[24] Das A, Chakraborty B, Sood AK. Raman spectroscopy of graphene on different substrates and influence of defects. Bull Mater Sci 2008;31(3):579–84.
[25] Prolongo S, Jimenez-Suarez A, Moriche R, Ureña A. In situ processing of epoxy composites reinforced with graphene nanoplatelets. Compos Sci Technol 2013;86:185–91.
[26] Mueller S, Llewellin EW, Mader HM. The rheology of suspensions of solid particles. Proc Roy Soc A: Math Phys Eng Sci 2010;466(2116):1201–28.
[27] Krieger Irvin M, Dougherty Thomas J. A mechanism for non-Newtonian flow in suspensions of rigid spheres. Trans Soc Rheol 1959;3:137–52.
[28] Corcione CE, Freuli F, Maffezzoli A. The aspect ratio of epoxy matrix nanocomposites reinforced with graphene stacks. Polym Eng Sci 2013;53(3):531–9.
[29] Monti M, Rallini M, Puglia D, Peponi L, Torre L, Kenny J. Morphology and electrical properties of graphene–epoxy nanocomposites obtained by different solvent assisted processing methods. Compos Part A: Appl Sci Manuf 2013;46:166–72.
[30] Li J, Kim J. Percolation threshold of conducting polymer composites containing 3D randomly distributed graphite nanoplatelets. Compos Sci Technol 2007;67(10):2114–20.
[31] Xie SH, Liu YY, Li JY. Comparison of the effective conductivity between composites reinforced by graphene nanosheets and carbon nanotubes. Appl Phys Lett 2008;92(24):243121.
[32] Jungki Seo JCSK. Enhancement of the thermal conductivity of adhesives for wood flooring using xGnP. Energy Build 2012:153–6.
[33] Yu A, Ramesh P, Itkis M, Bekyarova E, Haddon R. Graphite nanoplatelet–epoxy composite thermal interface materials. J Phys Chem C 2007;111(21):7565–9.
[34] Yu L, Park JS, Lim Y, Lee CS, Shin K, Moon HJ, et al. Carbon hybrid fillers composed of carbon nanotubes directly grown on graphene nanoplatelets for effective thermal conductivity in epoxy composites. Nanotechnology 2013;24(15):155604.
[35] Huang X, Zhi C, Jiang P. Toward effective synergetic effects from graphene nanoplatelets and carbon nanotubes on thermal conductivity of ultrahigh volume fraction nanocarbon epoxy composites. J Phys Chem C 2012;116(44):23812–20.
[36] Zhou S, Xu J, Yang Q, Chiang S, Li B, Du H, et al. Experiments and modeling of thermal conductivity of flake graphite/polymer composites affected by adding carbon-based nano-fillers. Carbon 2013;57:452–9.
[37] Fidelus J, Wiesel E, Gojny F, Schulte K, Wagner H. Thermo-mechanical properties of randomly oriented carbon/epoxy

nanocomposites. Compos Part A: Appl Sci Manuf 2005;36(11):1555–61.
[38] Starkova O, Chandrasekaran S, Prado L, Tölle F, Mülhaupt R, Schulte K. Hydrothermally resistant thermally reduced graphene oxide and multi-wall carbon nanotube based epoxy nanocomposites. Polym Degrad Stabil 2013;98(2):519–26.
[39] Srivastava I, Yu Z, Koratkar NA. Viscoelastic properties of graphene–polymer composites. Adv Sci Eng Med 2012;4(1):10–4.
[40] Starkova O, Buschhorn S, Mannov E, Schulte K, Aniskevich A. Water transport in epoxy/MWCNT composites. Eur Polym J 2013;49(8):2138–48.
[41] Swaminathan G, Shivakumar K. Thermomechanical and fracture properties of exfoliated nanoclay nanocomposites. J Reinforced Plast Compos 2011;30(3):256–68.
[42] Wang K, Chen L, Wu J, Toh ML, He C, Yee AF. Epoxy nanocomposites with highly exfoliated clay: mechanical properties and fracture mechanisms. Macromolecules 2005;38(3):788–800.
[43] Rafiee MA, Rafiee J, Srivastava I, Wang Z, Song H, Yu Z, et al. Fracture and fatigue in graphene nanocomposites. Small 2010;6(2):179–83.
[44] Tjong S. Structural and mechanical properties of polymer nanocomposites. Mater Sci Eng: R: Reports 2006;53(3–4):73–197.